

This article was downloaded by: [Pascal Morin]

On: 18 June 2012, At: 07:41

Publisher: Taylor & Francis

Informa Ltd Registered in England and Wales Registered Number: 1072954 Registered office: Mortimer House, 37-41 Mortimer Street, London W1T 3JH, UK



## International Journal of Control

Publication details, including instructions for authors and subscription information:

<http://www.tandfonline.com/loi/tcon20>

### Nonlinear complementary filters on the special linear group

Robert Mahony<sup>a</sup>, Tarek Hamel<sup>b</sup>, Pascal Morin<sup>c</sup> & Ezio Malis<sup>d</sup>

<sup>a</sup> Research School of Engineering, Australian National University, ACT 0200, Australia

<sup>b</sup> I3S UNSA-CNRS, 2000 route des Lucioles - Les Algorithmes - Bât. Euclide B, BP 121, 06903 Sophia Antipolis Cedex, France

<sup>c</sup> ISIR, UPMC, 75005 Paris Cedex 05, France

<sup>d</sup> ROBOCORTEX 35, Place des Cyprs, 06550 La Roquette sur Siagne, France

Available online: 11 Jun 2012

To cite this article: Robert Mahony, Tarek Hamel, Pascal Morin & Ezio Malis (2012): Nonlinear complementary filters on the special linear group, *International Journal of Control*, DOI:10.1080/00207179.2012.693951

To link to this article: <http://dx.doi.org/10.1080/00207179.2012.693951>



PLEASE SCROLL DOWN FOR ARTICLE

Full terms and conditions of use: <http://www.tandfonline.com/page/terms-and-conditions>

This article may be used for research, teaching, and private study purposes. Any substantial or systematic reproduction, redistribution, reselling, loan, sub-licensing, systematic supply, or distribution in any form to anyone is expressly forbidden.

The publisher does not give any warranty express or implied or make any representation that the contents will be complete or accurate or up to date. The accuracy of any instructions, formulae, and drug doses should be independently verified with primary sources. The publisher shall not be liable for any loss, actions, claims, proceedings, demand, or costs or damages whatsoever or howsoever caused arising directly or indirectly in connection with or arising out of the use of this material.

## Nonlinear complementary filters on the special linear group

Robert Mahony<sup>a\*</sup>, Tarek Hamel<sup>b</sup>, Pascal Morin<sup>c</sup> and Ezio Malis<sup>d</sup>

<sup>a</sup>Research School of Engineering, Australian National University, ACT 0200, Australia; <sup>b</sup>I3S UNSA-CNRS, 2000 route des Lucioles – Les Algorithmes – Bât. Euclide B, BP 121, 06903 Sophia Antipolis Cedex, France; <sup>c</sup>ISIR, UPMC, 75005 Paris Cedex 05, France; <sup>d</sup>ROBOCORTEX 35, Place des Cyprs, 06550 La Roquette sur Siagne, France

(Received 23 November 2011; final version received 11 May 2012)

This article proposes a nonlinear complementary filter for the special linear Lie-group  $SL(3)$  that fuses low-frequency state measurements with partial velocity measurements and adaptive estimation of unmeasured slowly changing velocity components. The obtained results have direct application on the problem of filtering a sequence of image homographies acquired from low-quality video data. The considered application motivates us to derive results that provide adaptive estimation of the full group velocity or part of the group velocity that cannot be measured from sensors attached to the camera. We demonstrate the performance of the proposed filters on real world homography data.

**Keywords:** nonlinear observer; complementary filter; special linear group  $SL(3)$

### 1. Introduction

A classical problem in computer vision and robotics is the computation of the homography mapping relating images of a planar scene viewed from two different locations. There are several well-known algorithms to numerically compute a homography estimate between two images (e.g. Hartley and Zisserman 2000; Ma, Soatto, Kosecka, and Sastry 2003). For these ‘classical’ algorithms there is no difference whether the two images considered are separately obtained or drawn from a video sequence. Zhang, Li, and Wu (2007) used image flow computed from a pair of images to compute the homographies, however, their algorithm still considers isolated pairs of images, even though these pairs of images must now be closely related, such as images drawn from a video sequence, in order to compute the flow field. It is of interest to ask if the homography estimation associated with a whole sequence of video images can be improved by more explicitly considering the temporal relationship between images, essentially by using an image motion model. This question is related to the problem of visual odometry, or estimation of the pose of a moving camera, using planar texture features (Dellaert, Thorpe, and Thrun 1998) or homography transformations (Wang, Yuan, Zou, and Zhou 2005; Mufti, Mahony, and Kim 2007; Scaramuzza and Siegwart 2008). Indeed, it is possible to explicitly reconstruct the

relative rigid body pose of two cameras from a pair of images of a planar scene (Faugeras and Lustman 1988; Malis and Vargas 2007). However, the mapping between relative rigid-body pose of the camera and an associated image homography is highly nonlinear and has ambiguities that may lead to singularities. There are a number of important applications emerging where it is the homography itself that is required and the estimation of the camera pose is unnecessary. Problems in image registration and removal of ‘shake’ from video sequences obtained from hand-held video cameras are one of the motivating examples for this article (Irani, Rousso, and Peleg 1994; Buehler, Bosse, and McMillan 2001; Cho, Kim, and Hong 2007). There are also algorithms in navigation of robotic vehicles (Fang, Dixon, Dawson, and Chawda 2005; Fraundorfer, Engels, and Nister 2007) and particularly unmanned aerial vehicles (Caballero, Merino, Ferruz, and Ollero 2007; Mondragón, Campoy, Martínez, and Olivares-Méndez 2010) that works directly with homography sequences. We also mention some of the classical results in the image-based visual servo control that works directly with homographies (Malis, Chaumette, and Boudet 1999; Deguchi 1998). Defining a filter directly on the set of homographies overcomes the limitations associated with representing the filter state as a rigid-body pose. The special linear group structure of the homographies (Benhimane and

\*Corresponding author. Email: Robert.Mahony@anu.edu.au

Malis 2007) provides a geometric state-space representation that suggests the applicability of recent tools in the nonlinear observer design (Mahony, Hamel, and Pflimlin 2008; Bonnabel, Martin, and Rouchon 2008a; Lageman, Trumppf, and Mahony 2010). Prior work, however, has been focused on the special orthogonal and special Euclidean groups, with applications in attitude and pose estimation for mobile vehicles (Tayebi and McGilvray 2006; Martin and Salaün 2008; Vasconcelos, Cunha, Silvestre, and Oliveira 2010). The authors know of no prior work, except some preliminary work of their own (Malis, Hamel, Mahony, and Morin 2009, 2010) that considers nonlinear filter design on the special linear group.

In this article, we provide a nonlinear complementary filter for a kinematic system on the special linear  $SL(3)$  Lie-group. As a first study, we consider abstract kinematics with respect to the natural geometry of  $SL(3)$ . The filter obtained has a natural complementary filtering interpretation, preserving the low-frequency component of the state measurement and fusing this with the high-frequency content of the integrated velocity measurement. We build a filter for the case where the group velocity is known and then extend this to estimate a constant but unknown group velocity, an effective solution even when the unknown velocity is slowly time varying, that is when the filter response is sufficiently fast compared to the group velocity variation. We prove almost global stability and local exponential stability around the desired equilibrium point of this filter. We consider the specific application of filtering a sequence of homographies where the state measurement is provided by any of a range of classical computer vision algorithm. We apply the algorithm proposed in this article to a sequence of real-world data, using the adaptive state to provide an estimate of the unknown group velocity. The results obtained demonstrate the robust performance of the proposed filter. We go on to consider the case where the homography sequence is generated by motion of a camera over a static scene. In this case we derive the mapping between rigid-body velocity and group velocity of the induced homography sequence and use this to develop a filter that uses body-fixed frame measurements of a rigid-body velocity. We extend this result to consider the case where the angular velocity is measured (for instance, by embedded MEMS gyroscope sensors mounted on the camera), but the linear translational velocity must be estimated. This case is related to the growing literature on inertial vision systems (Dias, Vinzce, Corke, and Lobo 2007). In this section we assume that both the vision and inertial system have been calibrated. We note that the calibration problem for inertial vision itself has been the topic of significant recent research (Lobo and Dias

2007; Hol, Schn, and Gustafsson 2010; Martinelli 2012) and we believe that the general approach taken in this article may have application to calibration problem, however, such an investigation is beyond the scope of this article. We consider two cases; first, when the linear velocity of the camera is constant in the inertial frame, and second, when the linear velocity is constant in the body-fixed frame. In both cases an adaptive term in the filter is used to estimate the component of the unknown group velocity associated with the linear velocity term and the unmeasured structure parameter while utilising the angular velocity measurement.

This article is organised into five sections followed by a short conclusion. After the introduction, Section 2 proposes the complementary filter on  $SL(3)$ , provides a preliminary stability analysis and briefly discusses the properties of the filtered estimate. Section 3 contains the main result of this article, providing the full stability analysis of the complementary filter with an adaptive estimation of unknown group velocity. Section 4 considers the application to smoothing a sequence of noisy homographies and provides experimental verification of the algorithm proposed in Section 3. Section 5 considers the question of filtering a sequence of homographies in more detail, in particular, taking into account the possibility that the rigid-body motion of the camera is modelled. Initially, we assume the full rigid-body velocity of the camera is available, and then later go on to consider two cases of interest, where the angular velocity of the camera is known and the linear velocity is assumed constant in either the inertial frame or the body-fixed frame. A short conclusion is also provided.

## 2. Nonlinear filter on $SL(3)$ with known group velocity

In this section, we consider the abstract question of design of a filter on the special linear group. The system kinematics are modelled as left-invariant dynamics on the Lie group  $SL(3)$  with group velocity  $A \in \mathfrak{sl}(3)$ . The resulting filter has the natural structure of a complementary filter.

The matrix representation of the special linear group

$$SL(3) = \{H \in \mathbb{R}^{3 \times 3} \mid \det(S) = 1\}$$

is the set of non-singular,  $3 \times 3$  matrices with unit determinant. It is an eight-dimensional embedded Lie-subgroup of  $GL(3)$  in the natural manner. The Lie-algebra  $\mathfrak{sl}(3)$  for  $SL(3)$  is the set of matrices with trace equal to zero,  $\mathfrak{sl}(3) = \{X \in \mathbb{R}^{3 \times 3} \mid \text{tr}(X) = 0\}$ .

The adjoint operator is a mapping  $\text{Ad} : SL(3) \times \mathfrak{sl}(3) \rightarrow \mathfrak{sl}(3)$  defined by

$$\text{Ad}_H X = HXH^{-1}, \quad H \in SL(3), \quad X \in \mathfrak{sl}(3).$$

For any two matrices  $A, B \in \mathbb{R}^{3 \times 3}$  the Euclidean matrix inner product and Frobenius norm are defined as

$$\langle\langle A, B \rangle\rangle = \text{tr}(A^T B), \quad \|A\| = \sqrt{\langle\langle A, A \rangle\rangle}.$$

Let  $\mathbb{P}$  denote the unique orthogonal projection of  $\mathbb{R}^{3 \times 3}$  onto  $\mathfrak{sl}(3)$  with respect to the inner product  $\langle\langle \cdot, \cdot \rangle\rangle$ . It is easily verified that

$$\mathbb{P}(H) := \left( H - \frac{\text{tr}(H)}{3} I \right) \in \mathfrak{sl}(3). \quad (1)$$

For any matrices  $G \in SL(3)$  and  $B \in \mathfrak{sl}(3)$  then  $\langle\langle B, G \rangle\rangle = \langle\langle B, \mathbb{P}(G) \rangle\rangle$  and hence

$$\text{tr}(B^T G) = \text{tr}(B^T \mathbb{P}(G)). \quad (2)$$

Consider the standard left invariant kinematics defined on  $SL(3)$

$$\dot{H} = HA \quad (3)$$

where  $H \in SL(3)$  and  $A \in \mathfrak{sl}(3)$  (Bonnabel et al. 2008a; Lageman, Mahony, and Trumppf 2008).

Consider an estimate  $\hat{H}(t) \in SL(3)$  of the true homography  $H(t)$ . Define a group error

$$\tilde{H} = \hat{H}^{-1} H. \quad (4)$$

The group error provides a natural measure to evaluate performance of the filter response. The error  $\tilde{H}$  converges to the identity element of the group  $I$  if and only if the observation  $\hat{H} \rightarrow H$  converges to the system state.

**Lemma 2.1:** Consider the group kinematics (3) and assume that the group velocity  $A \in \mathfrak{sl}(3)$  is measured. Let

$$\dot{\tilde{H}} = \hat{H} \text{Ad}_{\tilde{H}}(A - k\mathbb{P}(\tilde{H}^T(I - \tilde{H}))) \quad (5)$$

where  $k > 0$ . Then  $I$  is a locally exponentially stable equilibrium of the error  $\tilde{H}$ .

**Proof:** The error dynamics are obtained by differentiating  $\tilde{H}$

$$\begin{aligned} \dot{\tilde{H}} &= -\hat{H}^{-1} \dot{\hat{H}} \hat{H}^{-1} H + \hat{H}^{-1} \dot{H} \\ &= -\text{Ad}_{\tilde{H}}(A - k\mathbb{P}(\tilde{H}^T(I - \tilde{H}))) \tilde{H} + \tilde{H} A \\ &= k\tilde{H} \mathbb{P}(\tilde{H}^T(I - \tilde{H})). \end{aligned} \quad (6)$$

Consider the Lyapunov function

$$\mathcal{L} = \frac{1}{2} \|\tilde{H} - I\|^2 = \frac{1}{2} \text{tr}((\tilde{H} - I)^T (\tilde{H} - I)). \quad (7)$$

The derivative of  $\mathcal{L}$  along the solutions of (6) is

$$\begin{aligned} \dot{\mathcal{L}} &= \text{tr}((\tilde{H} - I)^T \dot{\tilde{H}}) \\ &= k \text{tr}((\tilde{H} - I)^T \tilde{H} \mathbb{P}(\tilde{H}^T(I - \tilde{H}))) \\ &= k \text{tr}((\tilde{H}^T(\tilde{H} - I))^T \mathbb{P}(\tilde{H}^T(I - \tilde{H}))). \end{aligned}$$

Using the fact that  $\mathbb{P}(\tilde{H}^T(I - \tilde{H})) \in \mathfrak{sl}(3)$  and recalling property (2), it follows

$$\begin{aligned} \dot{\mathcal{L}} &= k \text{tr}(\mathbb{P}(\tilde{H}^T(\tilde{H} - I))^T \mathbb{P}(\tilde{H}^T(I - \tilde{H}))) \\ &= -k \|\mathbb{P}(\tilde{H}^T(I - \tilde{H}))\|^2. \end{aligned}$$

It is easily verified that  $a\|\tilde{H} - I\|^2 < \|\mathbb{P}(\tilde{H}^T(I - \tilde{H}))\|^2 < b\|\tilde{H} - I\|^2$  in the neighbourhood of the identity matrix for some constants  $a$  and  $b$  and the result follows from standard Lyapunov theory (Khalil 1996).  $\square$

**Remark 1:** Lemma 2.1 could be strengthened to almost global asymptotic stability with an explicit characterisation of the unstable equilibrium using the results presented in Theorem 3.2 if required.

The filter (5) is of interest due to its complementary filtering characteristics as well as the almost global asymptotic stability properties proved in Lemma 2.1. Complementary filters are filters that fuse different measurements of a single signal together into an all pass estimate based on frequency criteria on the input signals (Mahony et al. 2008). In the standard scenario considered, the state measurement is corrupted by zero mean high-frequency noise. Thus, it is reliable and unbiased at low-frequency but noisy at high-frequency. In contrast, the forward integration of the group velocity is reliable at high-frequency due to the natural frequency roll-off associated with the integration process. Thus, the goal is to combine low-frequency information from the state measurement together with high-frequency information from the velocity measurement to obtain the estimate of the signal.

Since the proposed filter (5) is inherently nonlinear the frequency response of the filter can only be shown by analogy. Consider a first-order approximation

$$\hat{H}(t) \approx H(t)(I + X(t)), \quad X(t) \in \mathfrak{sl}(3)$$

of the filter  $\hat{H}$  along a systems trajectory  $H(t)$ . Note that with this definition  $\tilde{H} \approx I - X$  and  $\tilde{H}^{-1} \approx I + X$ . The linearisation of the error dynamics are  $\dot{\tilde{H}} \approx \frac{d}{dt}(I - X) = -\dot{X}$ . One has

$$\begin{aligned} \dot{X} &\approx -\dot{\tilde{H}} \\ &= k\tilde{H} \mathbb{P}(\tilde{H}^T(\tilde{H} - I)) \\ &\approx k(I - X) \mathbb{P}((I + X)^T(-X)) \\ &\approx -kX \end{aligned}$$

where second- and higher-order terms are discarded to obtain the linearisation. It follows that the error variation  $X(t)$  behaves like the output of a first-order ‘low-pass’ filter with roll-off frequency  $k \text{ rad s}^{-1}$ . This is the component of the complementary filter that implements the low-pass dependence on the state measurements  $X \approx I - \hat{H}^{-1}H$ . The filter Equation (5) can now be written as

$$\begin{aligned}\dot{\hat{H}} &= \hat{H} \text{Ad}_{\tilde{H}}(A + k\mathbb{P}(\tilde{H}^\top(\tilde{H} - I))) \\ &\approx \hat{H} \text{Ad}_{\tilde{H}}(A - kX)\end{aligned}$$

ignoring quadratic or higher order terms in  $X$ . The term  $A$  is the direct measurement (hence containing the high-frequency components) of group velocity while  $X$  is a low-pass filtered version of state error. The frequency tradeoff between the two signals can be tuned by adjusting the gain  $k$  that determines the low-frequency response of the error dynamics.

Although the above discussion is only an argument by analogy, the filter (5) demonstrates a strong frequency selectivity in practice, effectively combining state and velocity measurements to reduce high-frequency noise and avoid low-frequency time-varying offsets in the resulting state estimate. The integration of the velocity measurements is a crucial aspect of the complementary filtering approach and makes this approach distinct from, and significantly outperform, simple low-pass filtering of the measurement.

### 3. A complementary filter on $SL(3)$ that also estimates group velocity

In practice, a measurement for the group velocity  $A$  may not be available for injection into the filter dynamics. This is the case in the application to filtering homographies considered later in this article. The remainder of this article considers a number of different solutions to deal with an unknown group velocity. The first approach taken is to assume that the group velocity is constant. In practice, such an assumption would never be expected to hold explicitly, however, the filter will still function effectively in the case where the group velocity varies slowly compared to the transient response of the filter. We propose a filter that includes an adaptive estimate of the unknown group velocity and prove the local exponential stability of the full error dynamics. Thus, the proposed filter will track a slowly time-varying group velocity with a small error. This is a common principle used in observer and filter problems and the experimental results presented in Section 4 demonstrate the effectiveness of the approach.

**Assumption 3.1:** Assume that the velocity  $A \in \mathfrak{sl}(3)$  in Equation (3) is constant.

Define a second error signal

$$\tilde{A} = A - \hat{A}.$$

The goal of the filter design is to choose dynamics for  $\tilde{H}(t) \in SL(3)$  and  $\hat{A}(t) \in \mathfrak{sl}(3)$  such that the estimation errors  $(\tilde{H} - I)$  and  $\tilde{A}$  are globally asymptotically and locally exponentially stable to zero. In fact, we cannot fully guarantee the global asymptotic stability as we will find that the filter we propose has isolated unstable critical points in the error dynamics, however, we will be able to prove the almost global asymptotic stability.

Consider the following filter for  $H$  that satisfies (3)

$$\dot{\hat{H}} = \hat{H} \text{Ad}_{\tilde{H}}(\hat{A} - k_1\mathbb{P}(\tilde{H}^\top(I - \tilde{H}))), \quad \hat{H}(0) = \hat{H}_0, \quad (8a)$$

$$\dot{\hat{A}} = -k_2\mathbb{P}(\tilde{H}^\top(I - \tilde{H})), \quad \hat{A}(0) = \hat{A}_0, \quad (8b)$$

where  $k_1, k_2 > 0$  and  $\tilde{H}$  is given by (4). Given the above filter, the error dynamics for  $(\tilde{H}, \tilde{A}) = (\hat{H}^{-1}H, A - \hat{A})$  are easily verified to be

$$\dot{\tilde{H}} = \tilde{H}(\tilde{A} + k_1\mathbb{P}(\tilde{H}^\top(I - \tilde{H}))) \quad (9a)$$

$$\dot{\tilde{A}} = k_2\mathbb{P}(\tilde{H}^\top(I - \tilde{H})). \quad (9b)$$

**Theorem 3.2:** Consider the group kinematics given by (3) for a constant group velocity  $A$  (Assumption 3.1). Consider the filter given by (8a)–(8b), Then, for the error dynamics (9):

- (i) All solutions converge to  $E = E_s \cup E_u$  with

$$E_s = (I, 0)$$

$$E_u = \{(\tilde{H}_0, 0) : \tilde{H}_0 = \lambda(I + (\lambda^{-3} - 1)v v^\top), v \in S^2\}$$

where  $\lambda < 0$  is the unique real solution of the equation  $\lambda^3 - \lambda^2 + 1 = 0$ .

- (ii) The equilibrium point  $E_s = (I, 0)$  is locally exponentially stable.  
 (iii) Any point of  $E_u$  is an unstable equilibrium. More precisely, for any  $(\tilde{H}_0, 0) \in E_u$  and any neighbourhood  $\mathcal{U}$  of  $(\tilde{H}_0, 0)$ , there exists an  $(\tilde{H}_1, \tilde{A}_1) \in \mathcal{U}$  such that the solution of system (9) issued from  $(\tilde{H}_1, \tilde{A}_1)$  converges to  $E_s$ .

**Proof:** We will proceed item by item:

**Proof of part (i):** Let us consider the following candidate Lyapunov function:

$$\mathcal{L} = \frac{1}{2} \|\tilde{H} - I\|^2 + \frac{1}{2k_2} \|\tilde{A}\|^2. \quad (10)$$

The derivative of  $\mathcal{L}$  along the solutions of system (9) is

$$\begin{aligned} \dot{\mathcal{L}} &= \text{tr}\left((\tilde{H} - I)^\top \dot{\tilde{H}}\right) + \frac{1}{k_2} \text{tr}\left(\tilde{A}^\top \dot{\tilde{A}}\right) \\ &= \text{tr}\left((\tilde{H} - I)^\top \tilde{H}\tilde{A} + k_1(\tilde{H} - I)^\top \tilde{H}\mathbb{P}(\tilde{H}^\top(I - \tilde{H}))\right) \\ &\quad + \frac{k_2}{k_2} \text{tr}\left(\tilde{A}^\top \mathbb{P}(\tilde{H}^\top(I - \tilde{H}))\right). \end{aligned}$$

Recalling (2), one obtains

$$\begin{aligned} \dot{\mathcal{L}} &= k_1 \left\langle \mathbb{P}(\tilde{H}^\top(\tilde{H} - I)), \mathbb{P}(\tilde{H}^\top(I - \tilde{H})) \right\rangle \\ &\quad + \left\langle \tilde{A}, \mathbb{P}(\tilde{H}^\top(\tilde{H} - I)) + \mathbb{P}(\tilde{H}^\top(I - \tilde{H})) \right\rangle, \\ &= -k_1 \|\mathbb{P}(\tilde{H}^\top(\tilde{H} - I))\|^2. \end{aligned} \tag{11}$$

The derivative of the Lyapunov function is negative semi-definite, and equal to zero when  $\mathbb{P}(\tilde{H}^\top(I - \tilde{H})) = 0$ . Since  $\mathcal{L}$  goes to infinity for  $\|\tilde{H} - I\|$  unbounded, the error dynamics are bounded and exist for all time. The dynamics of the estimation error is autonomous and it follows from LaSalle's theorem that all solutions of this system converge to the largest invariant set contained in  $\{(\tilde{H}, \tilde{A}) : \mathbb{P}(\tilde{H}^\top(\tilde{H} - I)) = 0\}$ .

We now prove that, for system (9) with  $\mathbb{P}(\tilde{H}^\top(I - \tilde{H})) \equiv 0$ , the largest invariant set  $E$  contained in  $\{(\tilde{H}, \tilde{A}) | \mathbb{P}(\tilde{H}^\top(\tilde{H} - I)) = 0\}$  is equal to  $E_s \cup E_u$ . We need to show that the solutions of system (9) with  $\mathbb{P}(\tilde{H}^\top(I - \tilde{H})) \equiv 0$  consist of all fixed points of  $E_s \cup E_u$ . Note that  $E_s = (I, 0)$  is clearly contained in  $E$ . Consider a solution  $(\tilde{H}(t), \tilde{A}(t)) \in E_u$ . First, we deduce from (9) with  $\mathbb{P}(\tilde{H}^\top(I - \tilde{H})) \equiv 0$  that  $\tilde{A}(t)$  is identically zero on the invariant set  $E$  and therefore  $\tilde{A}$  is constant. We also deduce from (9) with  $\mathbb{P}(\tilde{H}^\top(I - \tilde{H})) \equiv 0$  that  $\dot{\tilde{H}} = \tilde{H}\tilde{A}$ . Note that at this point one cannot infer that  $\tilde{H}$  is constant.

Since  $\mathbb{P}(\tilde{H}^\top(\tilde{H} - I)) = 0$ , we have that

$$\tilde{H}^\top(\tilde{H} - I) = \frac{1}{3} \text{trace}(\tilde{H}^\top(\tilde{H} - I))I, \tag{12}$$

and hence  $\tilde{H} = \tilde{H}^\top \tilde{H} - \mu I$  for some  $\mu \in \mathbb{R}$  and  $\tilde{H}$  is a symmetric matrix. Therefore,  $\tilde{H}$  can be decomposed as

$$\tilde{H} = UDU^\top, \tag{13}$$

where  $U \in SO(3)$  and  $D = \text{diag}(\lambda_1, \lambda_2, \lambda_3) \in SL(3)$  is a diagonal matrix which contains the three real eigenvalues of  $\tilde{H}$ . Without loss of generality, let us suppose that the eigenvalues are in an increasing order,  $\lambda_1 \leq \lambda_2 \leq \lambda_3$ . Substituting (13) into (12), one obtains

$$D(D - I) = \frac{1}{3} \text{trace}(D(D - I))I.$$

Given that  $\det(D) = 1$ , the  $\lambda_i$ 's satisfy the following equations:

$$\lambda_1(1 - \lambda_1) = \lambda_2(1 - \lambda_2) \tag{14}$$

$$\lambda_2(1 - \lambda_2) = \lambda_3(1 - \lambda_3) \tag{15}$$

$$\lambda_3 = 1/(\lambda_1\lambda_2), \tag{16}$$

which can also be written as follows:

$$\lambda_1 - \lambda_2 = (\lambda_1 - \lambda_2)(\lambda_1 + \lambda_2) \tag{17}$$

$$\lambda_1 - \lambda_3 = (\lambda_1 - \lambda_3)(\lambda_1 + \lambda_3) \tag{18}$$

$$\lambda_3 = 1/(\lambda_1\lambda_2). \tag{19}$$

First of all, note that if  $\lambda_1 = \lambda_2 = \lambda_3$  then  $\lambda_1 = \lambda_2 = \lambda_3 = 1$ . This solution is associated with the equilibrium point  $E_s = (I, 0)$ .

If  $\lambda_1 = \lambda_2 < \lambda_3$  then

$$1 = \lambda_2 + \lambda_3 \tag{20}$$

$$\lambda_3 = 1/(\lambda_2^2), \tag{21}$$

where  $\lambda_2 \in (-1, 0)$  is the unique real solution of the equation  $\lambda_2^3 - \lambda_2^2 + 1 = 0$ . This solution is associated with the equilibrium set  $E_u$ .

If  $\lambda_1 < \lambda_2 = \lambda_3$  then

$$1 = \lambda_1 + \lambda_2 \tag{22}$$

$$\lambda_1 = 1/\lambda_2^2 \tag{23}$$

so that  $\lambda_2$  is also a solution of the equation  $\lambda_2^3 - \lambda_2^2 + 1 = 0$ . But this is impossible since we supposed  $\lambda_1 < \lambda_2$  and the solution of the equation is such that  $-1 < \lambda_2 < 0$  and  $0 < \lambda_1 = 1/\lambda_2^2 < 1$ .

If  $\lambda_1 \neq \lambda_2 \neq \lambda_3$ , then

$$1 = \lambda_1 + \lambda_2 \tag{24}$$

$$1 = \lambda_1 + \lambda_3 \tag{25}$$

$$\lambda_3 = 1/(\lambda_1\lambda_2), \tag{26}$$

which means that  $\lambda_2 = \lambda_3$ , a contradiction.

In conclusion,  $\tilde{H} \in E_u$  has two equal negative eigenvalues  $\lambda_1 = \lambda_2 = \lambda < 0$  ( $\lambda$  is the unique real solution of the equation  $\lambda^3 - \lambda^2 + 1 = 0$ ) and the third one is  $\lambda_3 = 1/\lambda^2$ . Writing the diagonal matrix  $D$  as follows:

$$D = \lambda(I + (\lambda^{-3} - 1)e_3e_3^\top)$$

and substituting this into Equation (13), the matrix for the second solution ( $\lambda_1 = \lambda_2$ ) can be expressed as follows:

$$\tilde{H} = \lambda(I + (\lambda^{-3} - 1)(Ue_3)(Ue_3)^\top).$$

We have shown that  $\tilde{H}$  must have the form

$$\tilde{H} = \lambda(I + (\lambda^{-3} - 1)v v^\top), \quad (27)$$

where  $v = Ue_3$  is a unitary vector,  $\|v\| = 1$  and  $\lambda$  is the unique real constant value that verifies the equation  $\lambda^3 - \lambda^2 + 1 = 0$ .

It remains to show that  $\tilde{A} = 0$  on  $E_u$ . Note that  $\tilde{H} = UDU^\top$  with  $D$ , a constant matrix with eigenvalues  $(\lambda, \lambda, 1/\lambda^2)$  where  $\lambda^3 - \lambda^2 + 1 = 0$ . It follows that  $\tilde{H} = -[\tilde{H}, Z]$  for some  $Z = -Z^\top$  possibly time-varying such that  $\dot{U} = \dot{Z}U$ , where  $[\tilde{H}, Z] = \tilde{H}Z - Z\tilde{H}$  is the Lie bracket. Since  $\dot{H} = \tilde{H}\tilde{A}$ , then

$$\tilde{H}\tilde{A} = -[\tilde{H}, Z] \quad (28)$$

and consequently, using the fact that  $\tilde{A}$  is constant, we have

$$\begin{aligned} \frac{d}{dt}\tilde{A} = 0 &= -\frac{d}{dt}\tilde{H}^{-1}[\tilde{H}, Z] \\ &= \tilde{H}^{-1}[\dot{\tilde{H}}, Z]\tilde{H}^{-1}[\tilde{H}, Z] - \tilde{H}^{-1}[[\dot{\tilde{H}}, Z], Z] \\ &\quad - \tilde{H}^{-1}[\tilde{H}, \dot{Z}]. \end{aligned}$$

Rearranging, one obtains

$$\begin{aligned} [\tilde{H}, \dot{Z}] &= [\tilde{H}, Z]\tilde{H}^{-1}[\tilde{H}, Z] - [[\tilde{H}, Z], Z] \\ &= -\tilde{H}Z\tilde{H}^{-1}Z\tilde{H} + Z\tilde{H}Z. \end{aligned}$$

It is easily verified that  $v^\top[\tilde{H}, \dot{Z}]v = 0$  where  $v$  is defined in (27). Then we compute<sup>1</sup>

$$\begin{aligned} v^\top[\tilde{H}, \dot{Z}]v &= v^\top(-\tilde{H}Z\tilde{H}^{-1}Z\tilde{H} + Z\tilde{H}Z)v \\ &= -\frac{1}{\lambda^4}v^\top Z\tilde{H}^{-1}Zv + v^\top Z\tilde{H}Zv \\ &= +\frac{1}{\lambda^5}\|Zv\|^2 - \lambda\|Zv\|^2 \\ &= \|Zv\|^2 \end{aligned}$$

since  $(\frac{1}{\lambda^5} - \lambda) \neq 0$ . It follows  $Zv = 0$  or that  $Z = \zeta v_\times$  for some  $\zeta \in \mathbb{R}$ , is where  $v_\times$  is the skew-symmetric matrix associated with the cross-product by  $v$ , i.e.  $v_\times y = v \times y$ , for all  $y$ . Substituting this into (28), it follows directly that  $\tilde{A} = 0$  since  $[\tilde{H}, v_\times] = 0$  and this concludes the proof of Part (i).

**Proof of part (ii):** We compute the linearisation of system (9) at  $E_s = (I, 0)$ . Let us define  $X_1$  and  $X_2$  as elements of  $\mathfrak{sl}(3)$  corresponding to the first-order approximations of  $\tilde{H}$  and  $\tilde{A}$  around  $(I, 0)$

$$\tilde{H} \approx (I + X_1), \quad \tilde{A} \approx X_2.$$

Substituting these approximations into (9) and discarding all terms quadratic or higher order in  $(X_1, X_2)$  yields

$$\begin{pmatrix} \dot{X}_1 \\ \dot{X}_2 \end{pmatrix} = \begin{pmatrix} -k_1 I_3 & I_3 \\ -k_2 I_3 & 0 \end{pmatrix} \begin{pmatrix} X_1 \\ X_2 \end{pmatrix}. \quad (29)$$

Since  $k_1, k_2 > 0$ , the linearised error system is exponentially stable. This proves the local exponential stability of the equilibrium  $(I, 0)$ .

**Proof of Part (iii):** It is easily verified that for  $(\tilde{H}, \tilde{A}) \in E_u$

$$\begin{aligned} \mathcal{L} &= \frac{1}{2}\|\tilde{H} - I\|^2 + \frac{1}{2k_2}\|\tilde{A}\|^2 \\ &= \frac{1}{2}\|D - I\|^2 = (\lambda - 1)^2 + \frac{1}{2}(\lambda^{-2} - 1)^2 \\ &=: \mathcal{L}_u > 0 \end{aligned} \quad (30)$$

is constant. To prove the desired result it is sufficient to show that for any point  $(\tilde{H}_0, 0) \in E_u$ , and any neighbourhood  $\mathcal{U}$  of this point, one can find  $(\tilde{H}_1, \tilde{A}_1) \in \mathcal{U}$  such that

$$\mathcal{L}(\tilde{H}_1, \tilde{A}_1) < \mathcal{L}_u. \quad (31)$$

Since  $\mathcal{L}$  is strictly non-increasing along trajectories and all solutions converge to  $E_s \cup E_u$ , then the solution originating at such a point must converge to  $E_s$ .

Let  $\tilde{H}(\cdot)$  denote a smooth curve on  $SL(3)$ , solution of  $\dot{\tilde{H}} = \tilde{H}C$  with  $C$ , a constant element of  $\mathfrak{sl}(3)$  that will be specified latter on. We also assume that  $(\tilde{H}(0), 0) \in E_u$ . Let  $f(t) = \|\tilde{H}(t) - I\|^2/2$  so that, by (10),  $\dot{f}(0) = \mathcal{L}_u$ . The first derivative of  $f$  is given by

$$\begin{aligned} \dot{f}(t) &= \text{tr}((\tilde{H}(t) - I)^\top \dot{\tilde{H}}(t)) \\ &= \text{tr}((\tilde{H}(t) - I)^\top \tilde{H}(t)C) \\ &= \langle \mathbb{P}(\tilde{H}^\top(t)(\tilde{H}(t) - I)), C \rangle. \end{aligned}$$

For all elements  $(\tilde{H}_0, 0) \in E_u$ , one has  $\mathbb{P}(\tilde{H}_0^\top(\tilde{H}_0 - I)) = 0$ , so that  $\dot{f}(0) = 0$ . We now calculate the second-order derivative of  $f$

$$\begin{aligned} \ddot{f}(t) &= \text{tr}(\dot{\tilde{H}}(t)^\top \dot{\tilde{H}}(t)) - \text{tr}((I - \tilde{H}(t))^\top \ddot{\tilde{H}}(t)) \\ &= \text{tr}(\dot{\tilde{H}}(t)^\top \dot{\tilde{H}}(t)) + \text{tr}((\tilde{H}(t) - I)^\top \ddot{\tilde{H}}(t)C), \end{aligned}$$

where we have used the fact that  $C$  is constant. Evaluating the above expression at  $t=0$  and replacing  $\tilde{H}(0)$  by its value  $\tilde{H}(0)C$  yields

$$\ddot{f}(0) = \|\tilde{H}(0)C\|^2 + \text{tr}((\tilde{H}(0) - I)^\top \tilde{H}(0)C^2). \quad (32)$$

When  $(\tilde{H}_0, 0) \in E_u$ , one has

$$\tilde{H}_0^2 = \lambda^2 I + \left(\frac{1}{\lambda^2} - \lambda\right)v v^\top = \tilde{H}_0 + (\lambda^2 - \lambda)I.$$

Therefore, we deduce from (32) that

$$\ddot{f}(0) = \|\tilde{H}(0)C\|^2 + \lambda(\lambda - 1)\text{tr}(C^2). \quad (33)$$

Since  $(\tilde{H}(0), 0) \in E_u$ , there exists a  $v \in \mathcal{S}^2$  such that  $\tilde{H}(0) = \lambda I + (\frac{1}{\lambda^2} - \lambda)vv^\top$ . From this expression and using the fact that  $\lambda^3 - \lambda^2 + 1 = 0$ , one verifies that

$$\|\tilde{H}(0)C\|^2 = \lambda^2\|C\|^2 + \left(\frac{1}{\lambda^2} - \lambda\right)\text{tr}(C^\top vv^\top C). \quad (34)$$

Setting  $C = v_\times \in \mathfrak{sl}(3)$ , it follows from (33) and (34) that

$$\begin{aligned} \ddot{f}(0) &= \lambda^2\|C\|^2 + \lambda(\lambda - 1)\text{tr}(C^2) \\ &= \lambda^2\text{tr}(v_\times^\top v_\times) + \lambda(\lambda - 1)\text{tr}((v_\times)^2) \\ &= -\lambda^2\text{tr}((v_\times)^2) + \lambda(\lambda - 1)\text{tr}((v_\times)^2) \\ &= -\lambda\text{tr}((v_\times)^2) = 2\lambda\|v\|^2 = 2\lambda < 0. \end{aligned}$$

Therefore, there exists a  $t_1 > 0$  such that for any  $t \in (0, t_1)$ ,

$$\begin{aligned} f(t) &\approx f(0) + tf'(0) + t^2/2\ddot{f}(0) \\ &\approx \mathcal{L}_u + t^2/2\ddot{f}(0) < \mathcal{L}_u. \end{aligned}$$

Equation (31) follows by setting  $(\tilde{H}_1, A_1) = (\tilde{H}(t), 0)$  with  $t \in (0, t_1)$  chosen small enough so as to have  $(\tilde{H}(t), 0) \in \mathcal{U}$ . This concludes the proof of Part (iii) and the proof of the theorem.  $\square$

#### 4. Complementary filtering for homographies

In this section, we consider the application of the results proposed in Sections 2 and 3 to the problem of tracking time-varying homographies.

A homography is a mapping between two images of a planar scene  $P$ . Let  $p = (u, v)$  represent the pixel coordinates of a 3D point  $x \in P$ , as observed in the normalised image plane of a pinhole camera. Let  $\mathcal{A}$  (resp.  $\mathcal{B}$ ) denote projective coordinates for the image plane of a camera  $A$  (resp.  $B$ ), and let  $\{A\}$  (resp.  $\{B\}$ ) denote its (right-hand) frame of reference. Any  $3 \times 3$  non-singular matrix,  $H$ , defines a homography mapping  $H : \mathcal{B} \rightarrow \mathcal{A}$ ,  $p^A = w(H, p^B)$ , by

$$w(H, p) = \begin{bmatrix} (h_{11}u + h_{12}v + h_{13})/(h_{31}u + h_{32}v + h_{33}) \\ (h_{21}u + h_{22}v + h_{23})/(h_{31}u + h_{32}v + h_{33}) \end{bmatrix}$$

with  $h_{ij}$  the entries of  $H$ . The mapping is only defined up to a scale factor; that is, for any scale factor  $\gamma \neq 0$ ,  $p^A = w(\gamma H, p^B) = w(H, p^B)$ .

Recall that the special linear Lie-group  $SL(3)$  is defined as the set of all real valued  $3 \times 3$  matrices with unit determinant

$$SL(3) = \{S \mid \det S = 1\}.$$

Since a homography matrix  $H$  is only defined up to scale, then any homography matrix is associated with a unique matrix  $H_* \in SL(3)$  by re-scaling

$$H_* = \frac{1}{\det(H)^{\frac{1}{3}}} H \quad (35)$$

such that  $\det(H_*) = 1$ . Moreover, the map  $w$  is a group action of  $SL(3)$  on  $R^2$

$$\begin{aligned} w(H_1, w(H_2, p)) &= w(H_1 H_2, p) \\ w(I, p) &= p, \end{aligned}$$

where  $H_1, H_2$  and  $H_1 H_2 \in SL(3)$  and  $I$  is the identity matrix. As a consequence, one may think of homographies as identified with the elements of  $SL(3)$ .

**Remark 2:** It is worth noting that a homography  $H$  does not in itself reference specific images  $\mathcal{A}$  and  $\mathcal{B}$ . The same homography may refer to different images taken with respect to different frames of reference. Indeed, if one fixes  $\mathcal{A}$  and considers only homographies that map to an arbitrary second image  $\mathcal{B}$ , then the resulting subset of all possible homographies is a proper subset of  $SL(3)$ .

The algorithm proposed in Theorem 3.2 was applied to a sequence of homographies obtained from real data. The data used for this experiment were obtained from a fully calibrated system. In the experiment, the user selects a rectangular area of interest in the first image. The homographies that transform the area of interest in the current image are measured using the ESM visual tracking software<sup>2</sup> (Benhimane and Malis 2007). Figure 1 shows four images extracted from the Corkes sequence. The first image in the figure shows a rectangle containing the area of interest that must be tracked in all the images of the video sequence. For each image of the sequence, the output of the ESM visual tracking algorithm is the homography that encodes the transformation of each pixels of the rectangular area from the current to the first image.

The measured homographies are the input of the proposed nonlinear filter. In this experiment the gains were  $k_1 = 5$  and  $k_2 = 1$ . The filtering effect of the filter on the estimated homography are visible in Figure 2. Note that the measurements have a level of jitter or noise that is smoothed in the filtered estimates. A key aspect of the proposed approach is that it provides estimates of the group velocity  $\dot{A}$  as a part of the filter process. The filter assumes that the group velocity is constant, however, as long as the velocity varies slowly with respect to the time constant of the filter then the filter provides an estimate of the homography velocity. The estimate of the group velocity is shown in Figure 3. This estimate is clearly superior to an estimate



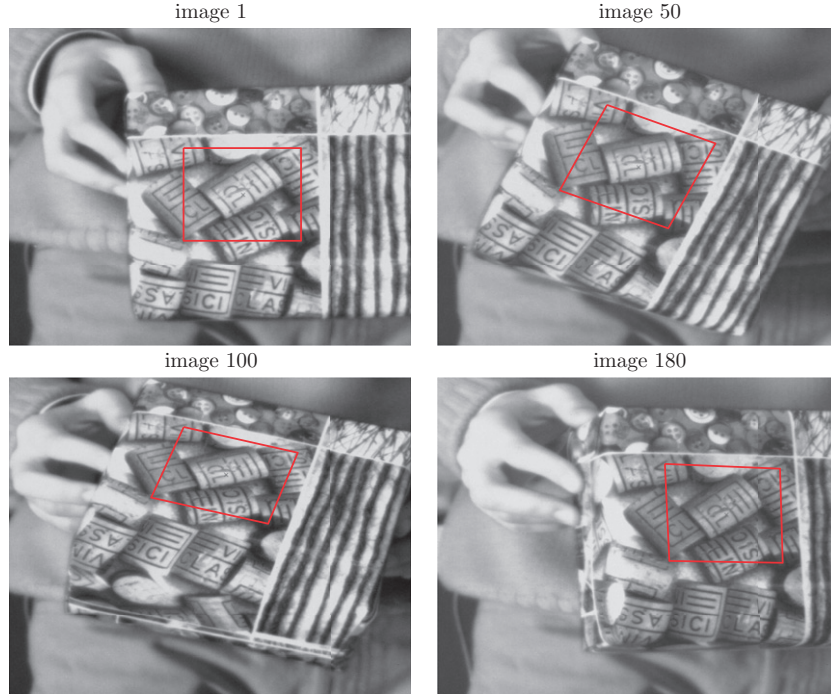


Figure 1. Images from the Corkes sequence. The quadrilateral in the centre of the first image indicates the image patch tracked in subsequent images. The visual tracking is correctly performed in real-time. However, the noise in the images and modelling errors affect the accuracy of the measured homographies.

obtained by differentiating the homography matrices directly. The estimation of the group velocity is potentially useful in image based control algorithms or in image compression algorithms.

### 5. Homography filter for a camera moving with rigid-body motion

In this section, we consider the case where the homographies considered are generated by a camera moving subject to rigid-body motion. The goal is to develop a nonlinear filter for the image homography sequence using the velocity associated with the rigid-body motion of the camera rather than the group velocity of the homography sequence, as was assumed in Section 4. This is an important consideration for applications where the velocity of the rigid-body motion of the camera is known or partly known from additional external sensors. For example, angular velocity can be measured using gyroscopes mounted on the camera, while in applications such as, for example, a camera fixed to an automobile or attached to a fixed-wing drone, the body-fixed frame direction of velocity is constrained and its magnitude is not difficult to measure. It is also of interest to consider the case of constant but with unknown rigid-body linear velocity, either in the body-fixed frame or inertial frame, as

these are common assumptions in many applications. These cases are treated in subsections following the main result of the section.

A homography can be related to the underlying rigid-body pose of the cameras with respect to the planar scene. We denote the attitude and position of  $\{B\}$  with respect to  $\{A\}$ , by  ${}^A R_B, {}^A \xi_B$ . A homography  $H$  mapping  $B$  to  $A$  can be written as (see Faugeras and Lustman (1988) for a numerical decomposition and Malis and Vargas (2007) for the analytical decomposition)

$$H = \gamma K \left( R + \frac{\xi n_B^\top}{d_B} \right) K^{-1} \quad (36)$$

where  $K$  is the upper triangular matrix containing the camera intrinsic parameters,  $R = {}^A R_B$  is the rotation matrix representing the orientation of  $\{B\}$  with respect to  $\{A\}$  expressed in  $\{A\}$ ,  $\xi = {}^A \xi_B$  is the translation vector of the origin of  $\{B\}$  with respect to  $\{A\}$  expressed in  $\{A\}$ ,  $n_B$  is the normal to the planar surface  $P$  expressed in  $\{B\}$ ,  $d_B$  is the orthogonal distance of the origin of  $\{B\}$  to the planar surface and  $\gamma$  is a scaling factor. Note that there exist multiple possible solutions to the decomposition (36) (Ma et al. 2003) that must be separately resolved by considering of physical constraints of the imaging system. The local parameterisation given by (36) is also singular when

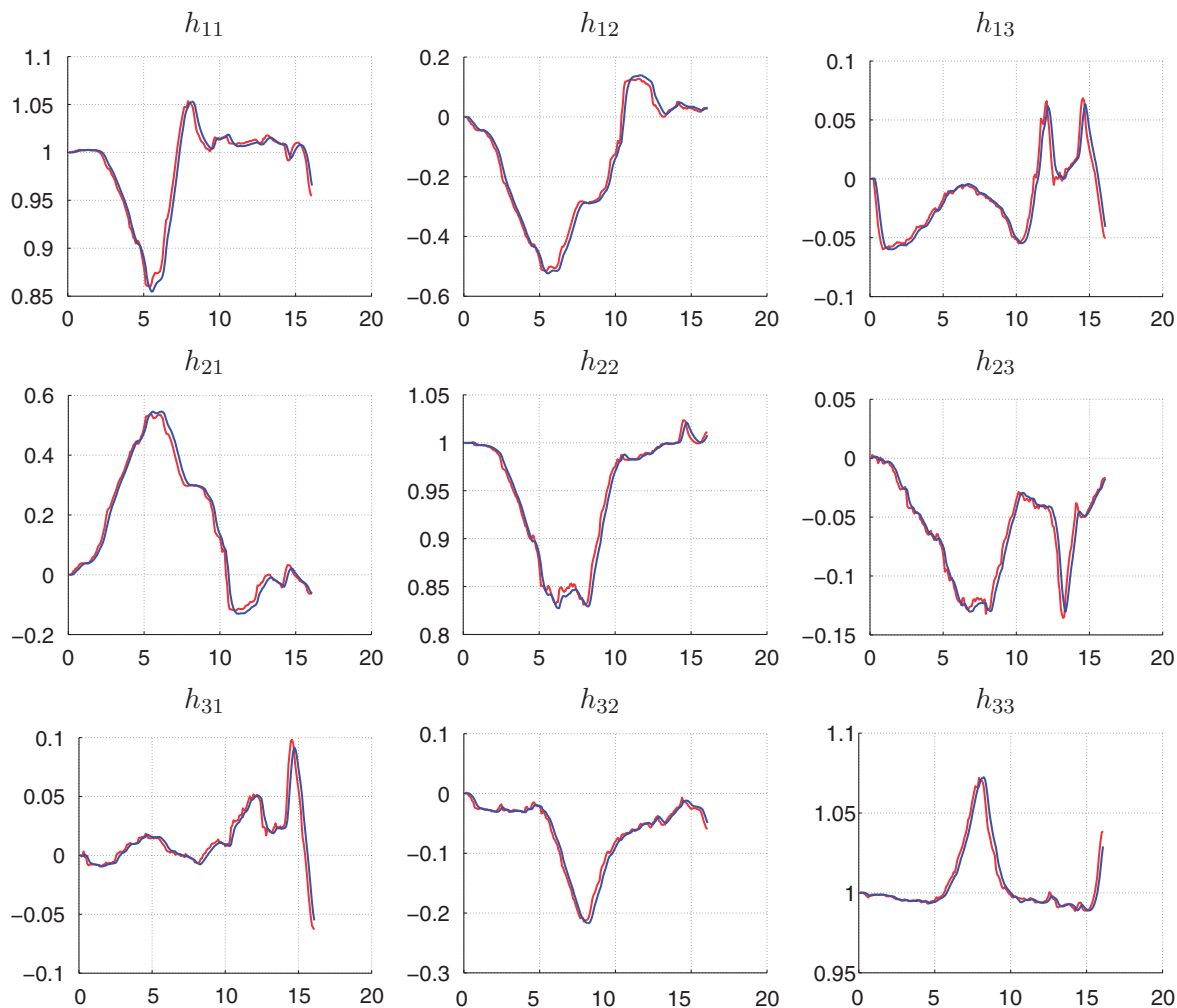


Figure 2. Corkes sequence. Each plot represents an element of the  $(3 \times 3)$  homography matrix. The leading line (red or lighter line): the measured homography matrix  $\bar{H}$ . The second (blue or darker) line: the observed homography  $\hat{H}$  lags slightly behind the noisier homography measurement due to the time variation of the velocity.

$\{A\}$  and  $\{B\}$  are collocated. That is, when  $\xi=0$ , the differential of the mapping,  $H \mapsto (R, \xi)$ , defined by (36) is degenerate. Indeed, in this case the normal,  $n_B$ , to the planar surface is not observable.

Denote the rigid-body angular velocity and linear velocity of  $\{B\}$  with respect to  $\{A\}$  expressed in  $\{B\}$  by  $\Omega = {}^B_A \Omega_B$  and  $V = {}^B_A V_B$ , respectively. The rigid body kinematics of  $(R, \xi)$  are given by

$$\dot{R} = R\Omega_{\times} \quad (37)$$

$$\dot{\xi} = RV \quad (38)$$

where  $\Omega_{\times}$  is the skew symmetric matrix associated with the vector cross-product, i.e.  $\Omega_{\times}y = \Omega \times y$ , for all  $y$ .

**Assumption 5.1:** Assume that the sequence of homographies are generated by a moving camera viewing a stationary planar surface.

This assumption imposes non-trivial constraints on the possible group velocities that can be attained. In particular, the assumption is equivalent to fixing the rigid-body pose of the camera in the reference position and fixing the planar scene stationary. Thus, any group velocity (infinitesimal variation of the homography) must be associated with instantaneous variation in measurement of the *active* image (due to motion of the rigid-body pose of the camera) and not variation in the *reference* image. This imposes constraints on two degrees of freedom in the homography velocity, in particular, those associated with the variation of the normal to the reference image, and leaves the remaining six degrees of freedom in the homography group velocity depending on the rigid-body velocities of the camera.

Let  $n$  denote the normal to the planar surface that is viewed by the camera. Then  $n_B$  is this normal

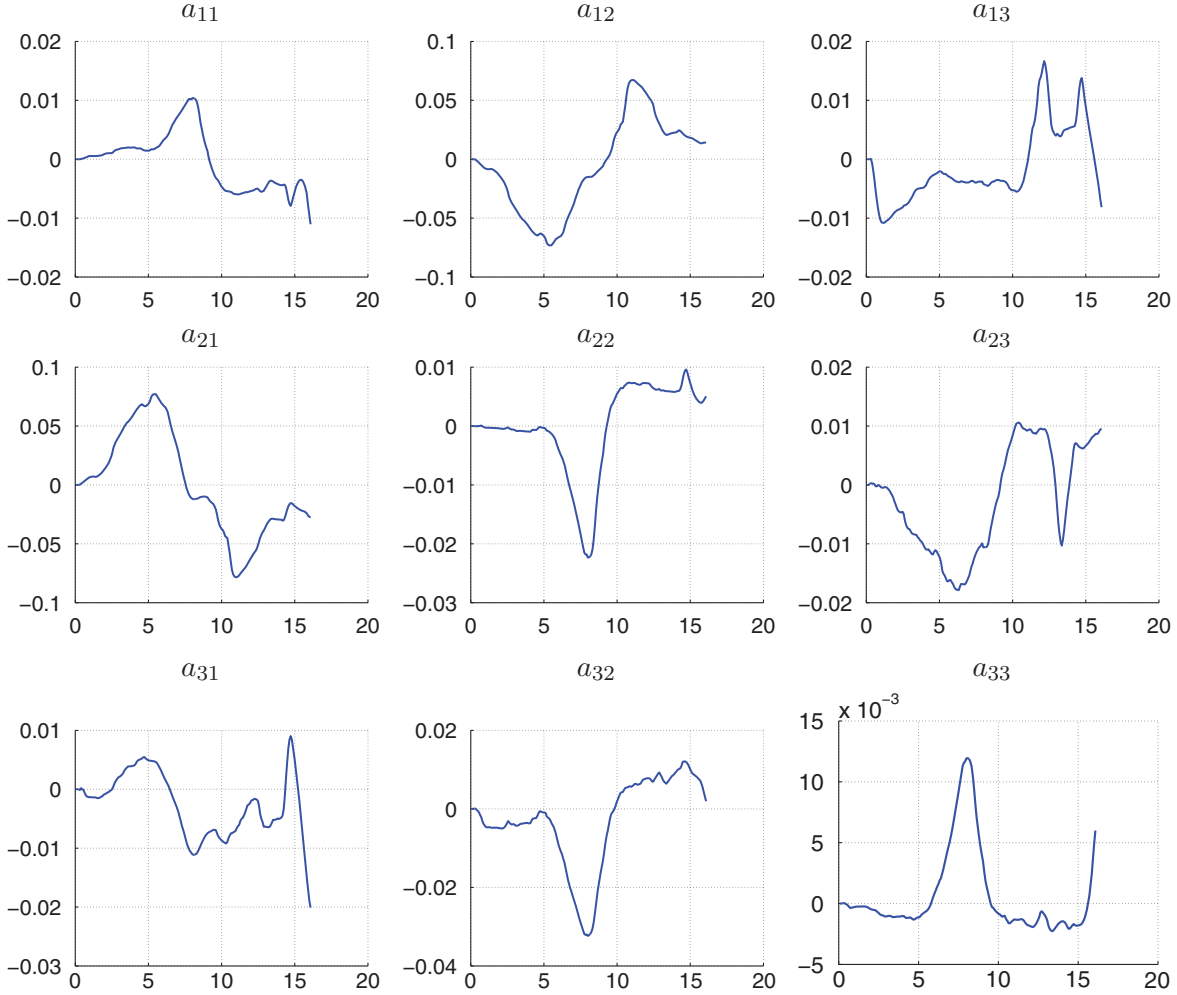


Figure 3. Corkes sequence. Each plot represents an element of the observed homography velocity matrix  $\hat{A}$ .

expressed in  $\{B\}$  and  $n_A = Rn_B$  is the same physical vector expressed in  $\{A\}$ . It is easily verified that

$$\dot{n}_B = -\Omega_\times n_B, \quad \dot{n}_A = 0 \quad (39)$$

This constraint on the variation of  $n_A$  and  $n_B$  is precisely the velocity constraint associated with Assumption 5.1.

The scalar  $d_B$  is the orthogonal distance of the origin of  $\{B\}$  to the planar surface while  $d_A$  is used to refer to the orthogonal distance from the origin of  $\{A\}$  to the surface. It is easily verified that

$$\dot{d}_B = -n_B^\top V, \quad \dot{d}_A = 0.$$

Although this equation appears to result in an additional constraint to the possible velocities of the homography, this is not the case since the relative scale constraint associated with variation in  $d_A$  is already absorbed in the scale invariance of the homography representation.

**Assumption 5.2:** Assume that the calibration matrix  $K$  for the considered camera is known.

For the remainder of this article, we will restrict our attention to the calibrated homography  $H = K^{-1}H_{\text{raw}}K$  where  $H_{\text{raw}}$  is the measured homography given by (36). That is,

$$H = K^{-1}H_{\text{raw}}K = \gamma \left( R + \frac{\xi n_B^\top}{d_B} \right) \quad (40)$$

where  $\gamma$  is the scale factor chosen such that  $\det(H) = 1$ .

**Lemma 5.3:** Consider a camera moving with kinematics (37) and (38) viewing a planar scene (Assumption 5.1). Let  $H : \mathcal{B} \rightarrow \mathcal{A}$  denote the calibrated homography (40). The group velocity  $A \in \mathfrak{sl}(3)$  such that  $\dot{H} = HA$  induced by the rigid-body motion is given by

$$A = \left( \Omega_\times + \frac{Vn_B^\top}{d_B} - \frac{n_B^\top V}{3d_B} I \right) \quad (41)$$

where  $n_B$  is the normal to the observed planar surface expressed in the camera frame  $\{B\}$  at time  $t$  and  $d_B$  is the orthogonal distance of the camera to the planar surface.

**Proof:** Consider the time derivative of (40). One has

$$\dot{H} = \gamma \left( \dot{R} + \frac{\dot{\xi} n_B^\top + \xi \dot{n}_B^\top}{d_B} - \frac{\dot{d}_B \xi n_B^\top}{d_B^2} \right) + \frac{\dot{\gamma}}{\gamma} H. \quad (42)$$

Recalling Equations (37) and (38), one has

$$\begin{aligned} \dot{H} &= \gamma \left( R \Omega_\times + \frac{R V n_B^\top + \xi n_B^\top \Omega_\times}{d_B} + \frac{n_B^\top V \xi n_B^\top}{d_B^2} \right) + \frac{\dot{\gamma}}{\gamma} H \\ &= \gamma \left( \left[ R + \frac{\xi n_B^\top}{d_B} \right] \Omega_\times + \left[ R + \frac{\xi n_B^\top}{d_B} \right] \frac{V n_B^\top}{d_B} \right) + \frac{\dot{\gamma}}{\gamma} H \\ &= H \left( \Omega_\times + \frac{V n_B^\top}{d_B} + \frac{\dot{\gamma}}{\gamma} I \right). \end{aligned}$$

Applying the constraint that  $\text{tr}(A) = 0$  for any element of  $\mathfrak{sl}(3)$ , one obtains

$$0 = \text{tr} \left( \Omega_\times + \frac{V n_B^\top}{d_B} + \frac{\dot{\gamma}}{\gamma} I \right) = \frac{n_B^\top V}{d_B} + \frac{3\dot{\gamma}}{\gamma}.$$

The result follows by substitution.  $\square$

Note that the group velocity  $A$  induced by camera motion depends on the additional variables  $n_B$  and  $d_B$  that define the scene geometry at time  $t$  as well as the scale factor  $\gamma$ . The scale factor  $\gamma$  can be computed from the calibrated homography matrix  $H$  by taking the second singular value (Ma et al. 2003, Lemma 5.18)

$$\gamma(t) := \sigma_2(H(t)). \quad (43)$$

An explicit formula for the calculation of  $\gamma$  is proposed in Malis and Vargas (2007). Thus, we will consider  $\gamma$  to be a measured variable. One has

$$\begin{aligned} \det(H) &= \gamma^3 \det \left( R + \frac{\xi n_B^\top}{d_B} \right) \\ &= \gamma^3 \det \left( I + \frac{R^\top \xi n_B^\top}{d_B} \right) \\ &= \gamma^3 \left( 1 + \frac{n_B^\top R^\top \xi}{d_B} \right). \end{aligned}$$

Since  $d_A = d_B + n_B^\top R^\top \xi$ , it follows that

$$\left( \frac{d_B}{d_A} \right) = \gamma^3$$

and  $\gamma$  can be used to provide information on the relative scale.

The scene parameters  $n_B$  and  $d_A$  remain unknown and unmeasurable variables. They must be taken into

account in the filter design. This leads to the first result of this section. In particular, let

$$N_B = \frac{n_B}{d_A},$$

Then, recalling (39), one has  $\dot{N}_B = -\Omega_\times N_B$  since  $d_A$  is constant. Define the filter as follows:

$$\begin{aligned} \dot{\hat{H}} &= \hat{H} \text{Ad}_{\tilde{H}} \left( \Omega_\times + \frac{1}{\gamma^3} V \hat{N}_B^\top - \frac{1}{3\gamma^3} (\hat{N}_B^\top V) I \right. \\ &\quad \left. - k_1 \mathbb{P}(\tilde{H}^\top (I - \tilde{H})) \right) \end{aligned} \quad (44)$$

$$\dot{\hat{N}}_B = -\Omega_\times \hat{N}_B - \frac{k_2}{\gamma^3} \mathbb{P}(\tilde{H}^\top (I - \tilde{H}))^\top V \quad (45)$$

where  $k_1, k_2 > 0$ . The variable  $\hat{N}_B \in \mathbb{R}^3$  is an estimate for  $N_B$ . Let  $\tilde{N}_B = N_B - \hat{N}_B$ , then the error dynamics for the system are

$$\dot{\tilde{H}} = \tilde{H} \left( \frac{1}{\gamma^3} \left( V \tilde{N}_B^\top - \frac{1}{3} (\tilde{N}_B^\top V) I \right) + k_1 \mathbb{P}(\tilde{H}^\top (I - \tilde{H})) \right), \quad (46)$$

$$\dot{\tilde{N}}_B = -\Omega_\times \tilde{N}_B + \frac{k_2}{\gamma^3} \mathbb{P}(\tilde{H}^\top (I - \tilde{H}))^\top V. \quad (47)$$

**Theorem 5.4:** Consider a camera moving with kinematics (37) and (38) viewing a planar scene (Assumption 5.1). Let  $H : \mathcal{B} \rightarrow \mathcal{A}$  denote the calibrated homography (40) (Assumption 5.2). Let  $\gamma$  be given by (43) and assume that  $\gamma$  is bounded above and below, that is there exists an  $0 < \epsilon < B < \infty$  such that  $\epsilon \leq \gamma \leq B$  for all time. Assume that the body-fixed frame velocities  $V = {}^B_A V_B$  and  $\Omega = {}^B_A \Omega_B$  are measured, bounded and persistently exciting in the sense that the time-varying linear system with the state matrix  $A(t)$  and measurement matrix  $C(t)$  given by

$$\begin{aligned} A(t) &= \begin{pmatrix} -k_1 I_9 & \frac{1}{\gamma^3} \left( \text{vec}(I_3) V^\top - \frac{1}{3} I_3 \otimes V \right) \\ \frac{k_2}{\gamma^3} (V^\top \otimes I_3) \mathbb{T} & -\Omega_\times \end{pmatrix} \\ C(t) &= (I_9 \quad 0_{9 \times 3}) \end{pmatrix} \quad (48)$$

is uniformly observable.<sup>4</sup> Assume in addition, that  $\dot{V}$  is bounded. Consider the filter dynamics (44) and (45), then the following points hold for the filter error dynamics (46)–(47):

(i) All solutions converge to  $E = E_s \cup E_u$  with

$$E_s = (I, 0)$$

$$E_u = \{(\tilde{H}_0, 0) : \tilde{H}_0 = \lambda(I + (\lambda^{-3} - 1)v v^\top), v \in S^2\}$$

where  $\lambda < 0$  is the unique real solution of the equation  $\lambda^3 - \lambda^2 + 1 = 0$ .

- (ii) The equilibrium point  $E_s = (I, 0)$  is locally exponentially stable.
- (iii) Any point of  $E_u$  is an unstable equilibrium. More precisely, for any  $(\tilde{H}_0, 0) \in E_u$  and any neighbourhood  $\mathcal{U}$  of  $(\tilde{H}_0, 0)$ , there exists an  $(\tilde{H}^1, \tilde{N}_B^1) \in \mathcal{U}$  such that the solution of system (9) issued from  $(\tilde{H}^1, \tilde{N}_B^1)$  converges to  $E_s$ .

**Proof:** The proof is inspired from that of Theorem 3.2, with the differences due to the fact that system (46)–(47) is not autonomous, and therefore LaSalle's invariance principle does not apply.

Consider the Lyapunov function

$$\mathcal{L} = \frac{1}{2} \|\tilde{H} - I\|^2 + \frac{1}{2k_2} \|\tilde{N}_B\|^2. \quad (49)$$

The derivative of  $\mathcal{L}$  is

$$\begin{aligned} \dot{\mathcal{L}} &= \text{tr} \left( (\tilde{H} - I)^\top \tilde{H} \left( \frac{1}{\gamma^3} \left( V \tilde{N}_B^\top - \frac{1}{3} (\tilde{N}_B^\top V) I \right) \right. \right. \\ &\quad \left. \left. + k_1 \mathbb{P}(\tilde{H}^\top (I - \tilde{H})) \right) \right) \\ &\quad + \frac{1}{k_2} \tilde{N}_B^\top \left( -\Omega_\times \tilde{N}_B + \frac{k_2}{\gamma^3} \mathbb{P}(\tilde{H}^\top (I - \tilde{H}))^\top V \right), \\ &= -k_1 \|\mathbb{P}(\tilde{H}^\top (I - \tilde{H}))\|^2 \end{aligned}$$

where we note that  $\tilde{N}_B^\top \Omega_\times \tilde{N}_B = 0$  since  $\Omega_\times$  is anti-symmetric and the inner products are taken on  $\mathfrak{sl}(3)$ . Given that  $V, \Omega$  are bounded, it is easily verified that  $\dot{\mathcal{L}}$  is uniformly continuous and Barbalat's lemma can be used to prove the asymptotic convergence of  $\mathbb{P}(\tilde{H}^\top (I - \tilde{H})) \rightarrow 0$ .

**Proof of part (i):** Let

$$E_u^H = \{ \tilde{H} \in SL(3) \mid H = \lambda(I + (\lambda^{-3} - 1)v v^\top), v \in S^2 \}. \quad (50)$$

Then the convergence of  $\mathbb{P}(\tilde{H}^\top (I - \tilde{H}))$  to zero and boundedness of  $\tilde{H}$  imply, as in the case of Theorem 3.2, that either  $\tilde{H} \rightarrow I$  or  $\tilde{H} \rightarrow E_u^H$  and it remains to show that  $\tilde{N}_B$  converges to zero. First, note that  $\|\tilde{H} - I\|$  converges to a constant value  $\ell_0$ . We have  $\ell_0 = 0$  if  $\tilde{H}$  converges to the identity and  $\ell_0 = \mathcal{L}_u$  given by (30) if  $\tilde{H}$  converges to  $E_u^H$ . Since  $\mathcal{L}$  is decreasing and positive,  $\mathcal{L}$  converges to a constant value so that  $\|\tilde{N}_B\|$  also converges to a constant value.

Note that, if  $\tilde{H}$  converges to  $I$  then  $\dot{\tilde{H}}$  converges to zero because  $\tilde{H}$  is uniformly continuous, since  $\dot{V}$  is bounded. Thus, from (46) one has

$$\lim_{t \rightarrow \infty} \left( V \tilde{N}_B^\top - \frac{1}{3} (\tilde{N}_B^\top V) I \right) = 0.$$

Since both  $V$  and  $\tilde{N}_B$  are bounded then continuity ensures that

$$\begin{aligned} \lim_{t \rightarrow \infty} \left[ V^\top \left( V \tilde{N}_B^\top - \frac{1}{3} (\tilde{N}_B^\top V) I \right) \tilde{N}_B \right] \\ = \left( \|V\|^2 \|\tilde{N}_B\|^2 - \frac{1}{3} (\tilde{N}_B^\top V)^2 \right) = 0. \quad (51) \end{aligned}$$

Applying the Cauchy–Schwartz inequality, it follows that  $\|V\| \|\tilde{N}_B\|$  converges asymptotically to zero. Since  $\|\tilde{N}_B\|$  converges to a constant and  $V$  is persistently exciting, one concludes that  $\tilde{N}_B$  converges to zero and the set  $E_s = \{(I, 0)\}$  is locally asymptotically stable.

It remains to show that the only other possibility is that the error system  $(\tilde{H}, \tilde{N}_B)$  converges to  $E_u$ . The proof proceeds by contradiction. Assume that  $(\tilde{H}, \tilde{N}_B) \not\rightarrow E_u \cup E_s$ . Then since the solution is bounded and exists for all time, and consequently evolves on a compact set, there exists limit points  $(\tilde{H}_*, \tilde{N}_*)$  and an unbounded increasing sequence of times  $t_n$  such that

$$\begin{aligned} \lim_{n \rightarrow \infty} \tilde{H}(t_n) &= \tilde{H}_* \in E_u^H, \\ \lim_{n \rightarrow \infty} \tilde{N}_B(t_n) &= \tilde{N}_* \neq 0. \end{aligned}$$

The first of these conditions follows from the Lyapunov argument that shows that if  $\tilde{H} \not\rightarrow I$  then  $\tilde{H} \rightarrow E_u^H$  while the second is the consequence of the assumption that we wish to contradict.

Without loss of generality choose the sequence  $t_n$  such that  $\inf_n \{t_{n+1} - t_n\} > 0$ . Then there exists a  $\delta > 0$  and two sequences of strictly increasing times  $\{a_n\}$  and  $\{b_n\}$  with

$$\dots < a_n < t_n < b_n < a_{n+1} < t_{n+1} < b_{n+1} < \dots$$

with  $b_n - a_n = \delta > 0$ . Define a sequence of functions

$$\tilde{H}_n : [-\delta/2, \delta/2] \rightarrow SL(3), \quad \tilde{H}_n(\tau) := \tilde{H}(\tau + a_n).$$

Due to the smooth definition of the system and bounded nature of the inputs, the sequence of functions  $\tilde{H}_n$  are smooth bounded functions defined on a compact interval. From the Arzelà–Ascoli theorem, possibly taking a subsequence of times, there exists a smooth function  $\tilde{H}_*(\tau) = \lim_{n \rightarrow \infty} \tilde{H}_n(\tau)$  with  $\tilde{H}_*(0) = \tilde{H}_*$  by construction. Moreover, it is straightforward to verify that  $\tilde{H}_*(t) \in E_u^H$  for  $t \in [-\delta/2, \delta/2]$ . To save the notation, we rely on context to distinguish between the limit function  $\tilde{H}_*(\tau)$  and limit point  $\tilde{H}_*$ .

Next choose a sequence of smooth vector-valued functions  $\{v_0^n(t), v_1^n(t), v_2^n(t)\}$  defined on the closed time intervals  $[-\delta/2, \delta/2]$  that are normalised eigenvectors of  $\tilde{H}_n(t)$  and such that

$$\lim_{n \rightarrow \infty} v_i^n(0) = v_i^*, \quad \text{for } i = 0, 1, 2,$$

where  $\{v_0^*, v_1^*, v_2^*\}$  is a set of orthonormal eigenvectors for  $\tilde{H}_*(t)$  such that  $\tilde{H}_* = \lambda(I + (\lambda^{-3} - 1)v_0^*v_0^{*\top})$ . Applying the Arzelà–Ascoli theorem again, and taking a suitable subsequence, the smooth functions  $\{v_0^n(t), v_1^n(t), v_2^n(t)\}$ , each thought of as a function from  $[-\delta/2, \delta/2]$ , have limits

$$\lim_{n \rightarrow \infty} v_i^n(t) = v_i^*(t)$$

with  $v^*(t)$  differentiable on  $(-\delta/2, \delta/2)$ . By continuity one has that  $\{v_0^*(t), v_1^*(t), v_2^*(t)\}$  are a set of orthonormal eigenvectors for  $\tilde{H}_*(t)$  such that  $\tilde{H}_*(t) = \lambda(I + (\lambda^{-3} - 1)v_0^*(t)v_0^*(t)^\top)$ . Finally, we will also need the two sequence of functions

$$\begin{aligned} \tilde{N}_B^n &: [-\delta/2, \delta/2] \rightarrow SL(3), & \tilde{N}_B^n(\tau) &:= \tilde{N}_B(\tau + a_n) \\ V^n &: [-\delta/2, \delta/2] \rightarrow SL(3), & V^n(\tau) &:= V(\tau + a_n). \end{aligned}$$

Using continuity and regularity and recalling that all the considered functions are defined on a compact interval  $[-\delta/2, \delta/2]$ , one has, for any  $i=0, 1, 2$ ,

$$\begin{aligned} \lim_{n \rightarrow \infty} \left( \frac{d}{dt} v_i^{n\top} \tilde{H}_n v_i^n \right) &= \frac{d}{dt} \lim_{n \rightarrow \infty} (v_i^{n\top} \tilde{H}_n v_i^n) \\ &= \frac{d}{dt} v_i^{*\top} \tilde{H}_* v_i^* = 0 \end{aligned}$$

where the final equality follows since  $v_i^*$  is an eigenvector of  $\tilde{H}_*$  with a constant eigenvalue. Computing the same limit but taking the derivative first yields

$$\begin{aligned} \lim_{n \rightarrow \infty} \frac{d}{dt} v_i^{n\top} \tilde{H}_n v_i^n &= \lim_{n \rightarrow \infty} \frac{1}{\gamma^3} v_i^{n\top} \tilde{H}_n \left( V^n \tilde{N}_B^{n\top} - \frac{1}{3} \tilde{N}_B^{n\top} V^n I \right) v_i^n \\ &= \lim_{n \rightarrow \infty} \frac{\text{const}}{\gamma^3} \tilde{N}_B^{n\top} \left( \frac{1}{3} I - v_i^n v_i^{n\top} \right) V^n \end{aligned}$$

with ‘const’ a non-zero constant which depends on  $i$ . This implies that for all  $i$ ,

$$\lim_{n \rightarrow \infty} \frac{1}{3} \tilde{N}_B^{n\top} V^n = \lim_{n \rightarrow \infty} \tilde{N}_B^{n\top} v_i^n(t_n) v_i^n(t_n)^\top V^n. \quad (52)$$

Analogously to above, one has

$$\lim_{n \rightarrow \infty} \frac{d}{dt} (v_1^{n\top} \tilde{H}_n v_2^n) = \frac{d}{dt} (v_1^{*\top} \tilde{H}_* v_2^*) = 0.$$

Since  $v_1^*$  and  $v_2^*$  are orthogonal vectors associated with the same eigenvalue  $\lambda$ , taking the derivative before the limit, one has

$$\begin{aligned} \lim_{n \rightarrow \infty} \frac{d}{dt} (v_1^{n\top} \tilde{H}_n v_2^n) &= \lim_{n \rightarrow \infty} \frac{1}{\gamma^3} v_1^{n\top} \tilde{H}_n \left( V^n \tilde{N}_B^{n\top} - \frac{1}{3} \tilde{N}_B^{n\top} V^n \right) v_2^n \\ &= \lim_{n \rightarrow \infty} \frac{\text{const}}{\gamma^3} \tilde{N}_B^{n\top} v_2^n v_1^{n\top} V^n = 0 \end{aligned} \quad (53)$$

and vice versa with the indices reversed. Now multiplying (52) together for  $i=1$  and  $i=2$  and using (53), one obtains

$$\lim_{n \rightarrow \infty} \frac{1}{9} \left( \tilde{N}_B^{n\top} V^n \right)^2 = 0 \quad (54)$$

or that  $\lim_{n \rightarrow \infty} \tilde{N}_B^{n\top} V^n = 0$ .

Recalling (46), and exploiting regularity of the solutions and limits, one has

$$\begin{aligned} \lim_{n \rightarrow \infty} \tilde{H}_n^{-1} \dot{\tilde{H}}_n v_0^n &= \tilde{H}_*^{-1} \frac{d}{dt} \tilde{H}_* v_0^* \\ &= \lambda^{-1} \left( I + (\lambda^{-3} - 1)v_0^*v_0^{*\top} \right)^{-1} \lambda(\lambda^{-3} - 1) \\ &\quad \times \left( \dot{v}_0^*v_0^{*\top} + v_0^*\dot{v}_0^{*\top} \right) v_0^* \\ &= \left( I + (\lambda^{-3} - 1)v_0^*v_0^{*\top} \right)^{-1} (\lambda^{-3} - 1)\dot{v}_0^* \\ &= (\lambda^{-3} - 1)\dot{v}_0^* \end{aligned} \quad (55)$$

since  $v_0^*$  and  $\dot{v}_0^*$  are orthogonal and  $v_0^*$  is a unit vector. A similar argument shows that

$$\lim_{n \rightarrow \infty} \tilde{H}_n^{-1} \dot{\tilde{H}}_n v_0^n = \lambda^3(\lambda^{-3} - 1)\|\dot{v}_0^*\|^2 v_0^*.$$

On the other hand, from (54) and (46) one has

$$\lim_{n \rightarrow \infty} \tilde{H}_n^{-1} \dot{\tilde{H}}_n w^n = \lim_{n \rightarrow \infty} \frac{1}{\gamma^3} V^n \tilde{N}_B^{n\top} w^n \quad (56)$$

for any sequence of functions  $w^n$  with a limit. It follows that

$$\begin{aligned} (\lambda^{-3} - 1)\dot{v}_0^* &= \lim_{n \rightarrow \infty} \frac{1}{\gamma^3} (\tilde{N}_B^{n\top} v_0^*) V^n \\ \lambda^3(\lambda^{-3} - 1)\|\dot{v}_0^*\|^2 v_0^* &= \lim_{n \rightarrow 0} \frac{1}{\gamma^3} (\tilde{N}_B^{n\top} \dot{v}_0^*) V^n. \end{aligned}$$

Since  $V^n \neq 0$  due to the persistence of excitation assumption, and noting that  $(v_0^*)^\top \dot{v}_0^* = 0$ , the only way that these equations can hold is if  $\dot{v}_0^* = 0$ . It follows that  $\lim_{n \rightarrow \infty} \tilde{H}_n = 0$ . From here, it follows that a version of Equation (51) holds for the functions  $\tilde{N}_B^n$  and  $V^n$  and the Cauchy–Schwarz inequality can be used to show

$$\lim_{n \rightarrow \infty} \tilde{N}_B^n = \tilde{N}_* = 0.$$

This contradicts the assumption and concludes part (i) of the proof.

**Proof of part (ii):** The linearisation of (46) and (47) around  $(\tilde{H}, \tilde{N}_B) = (I, 0)$  is given by

$$\begin{aligned} \dot{X} &= -k_1 X + \frac{1}{\gamma^3} V z^\top - \frac{1}{3\gamma^3} (z^\top V) I \\ \dot{z} &= -\Omega_\times z + \frac{k_2}{\gamma^3} X^\top V, \end{aligned}$$

where  $\tilde{H} \approx I + X$ ,  $X \in \mathfrak{sl}(3)$  and  $z \approx \tilde{N} \in \mathbb{R}^3$ . Taking the vec of this equation and writing  $x = \text{vec}(X)$  yields

$$\begin{pmatrix} \dot{x} \\ \dot{z} \end{pmatrix} = \begin{pmatrix} -k_1 I_9 & \frac{1}{\gamma^3} \left( \text{vec}(I_3) V^\top - \frac{1}{3} I_3 \otimes V \right) \\ \frac{k_2}{\gamma^3} (V^\top \otimes I_3) \mathbb{T} & -\Omega_\times \end{pmatrix}. \quad (57)$$

This linear system (that is known to be asymptotically stable from part (i) since  $E_s$  is isolated) is exponentially stable if the associated linear system with output  $y = x$  is uniformly observable (Khalil 1996). The condition imposed for the persistence of excitation in the theorem statement (48) completes the proof for part (ii).

**Proof of part (iii):** This result follows from part (iii) of Theorem 3.2. Indeed, it was proved that for any  $(\tilde{H}_0, 0) \in E_u = \{(\tilde{H}_0, 0) : \tilde{H}_0 = \lambda(I + (\lambda^{-3} - 1)v v^\top), v \in S^2\}$ , and any neighbourhood  $\mathcal{U}$  of this point, there exists an  $(\tilde{H}_1, A_1) = (\tilde{H}_1, 0) \in \mathcal{U}$  such that  $\mathcal{L}(\tilde{H}_1, A_1) < \mathcal{L}_u$ , with  $\mathcal{L}_u$  the value of  $\mathcal{L}$  on  $E_u$  and  $\mathcal{L}$  the Lyapunov function (10). Now taking the Lyapunov function (49) used in the present proof, it follows that  $\mathcal{L}(\tilde{H}_1, 0) < \mathcal{L}_u$  where  $\mathcal{L}_u$  is also the value of this function on  $E_u$ . Instability of this set follows from the fact that  $\mathcal{L}$  is decreasing along the system solutions.  $\square$

The persistence of excitation condition (48) on the velocity in Theorem 5.4 appears somewhat obscure, however, it is satisfied in almost all situations. If  $V$  is uniformly zero, then the homography sequence degenerates to a pure rotation and it is known that the normal to the reference plane cannot be determined from the homography (Faugeras and Lustman 1988; Malis and Vargas 2007). This property manifests as a loss of observability in (48). Considering (48) it is clear that as long as  $V(t)$  is sufficiently ‘non-zero’ in some uniform sense, the resulting linear system will be uniformly observable for bounded  $\gamma$  and independent of the signal  $\Omega$ . We believe it is most natural to think of this condition (uniform observability of (48)) as a persistence of excitation condition on the velocities, in this case really just a condition on  $V$ . The upper bound on  $\gamma$  in the theorem statement is also linked to the loss of uniform observability of (48). Physically,  $\gamma \rightarrow \infty$  corresponds to the camera moving infinitely far away from the planar target while the corresponding homography converges to a pure rotation in which information on the reference normal is unobservable. The bound  $\gamma > \epsilon > 0$  is more direct since  $\gamma \rightarrow 0$  corresponds to the camera intersecting the observed plane and leading to a singularity in the homography representation.

In the remaining two subsections we will consider the cases where the linear velocity of the vehicle is

unknown and constant, either in the body-fixed frame or in the inertial frame.

### 5.1 Constant linear velocity in the body-fixed frame

In this subsection we consider the case where the linear velocity is unknown but constant in the body-fixed frame. We will assume as before that the angular velocity in the body-fixed frame is measured. This is a common scenario in the motion of velocity-controlled non-holonomic robotic vehicles. In this case non-holonomic constraints typically constrain the vehicle to move in a fixed direction in the body-fixed frame, for example a unicycle mobile robot. If it is assumed in addition that the speed of the vehicle is constant then one has the case considered in this subsection. This class of system includes, at least approximately, a wide range of interesting real-world systems such as cars, and to a first approximation, fixed wing UAV drones and surface vessels, etc. There are a range of applications where homographies are used in the navigation and control of robotic vehicles (Fraundorfer et al. 2007) and especially unmanned aerial vehicles (Caballero et al. 2007; Mondragóon et al. 2010) where due to the height of the vehicle the planar scene constraint is usually approximately satisfied.

**Corollary 5.5:** *Consider a camera moving with kinematics (37) and (38) viewing a planar scene (Assumption 5.1). Let  $H : \mathcal{B} \rightarrow \mathcal{A}$  denote the calibrated homography (40) (Assumption 5.2). Let  $\gamma$  be given by (43) and assume that  $\gamma$  is bounded above and below, that is there exists an  $0 < \epsilon < B < \infty$  such that  $\epsilon \leq \gamma \leq B$  for all time. Assume that the body-fixed frame velocities  $\Omega = {}^B_A \Omega_B$  is measured, uniformly continuous, bounded and persistently exciting signal. Assume that the body-fixed linear velocity is constant and unknown*

$$V = {}^B_A V_B = \text{const.}$$

Let  $M = (1/d_A) V n_B^\top$  and let

$$\dot{\hat{H}} = \hat{H} \text{Ad}_{\tilde{H}} \left( \Omega_\times + \frac{1}{\gamma^3} \hat{M} - \frac{1}{3\gamma^3} \text{tr}(\hat{M}) I - k_1 \mathbb{P}(\tilde{H}^\top (I - \tilde{H})) \right) \quad (58)$$

$$\dot{\hat{M}} = \hat{M} \Omega_\times - \frac{k_2}{\gamma^3} \mathbb{P}(\tilde{H}^\top (I - \tilde{H})) \quad (59)$$

where  $k_1, k_2 > 0$ . Then the dynamics of  $(\tilde{H}, \tilde{M}) = (\hat{H}^{-1} H, M - \hat{M})$  satisfy properties (i), (ii) and (iii) in Theorem 5.4 with a suitable interpretation of the sets  $E_u$  and  $E_s$ .

**Proof:** It is straightforward to verify that

$$\dot{M} = M\Omega_\times.$$

Differentiating the estimation error  $(\tilde{H}, \tilde{M}) = (\hat{H}^{-1}H, M - \hat{M})$ , one obtains

$$\dot{\tilde{H}} = \tilde{H} \left( \frac{1}{\gamma^3} \tilde{M} - \frac{1}{3\gamma^3} \text{tr}(\tilde{M})I + k_1 \mathbb{P}(\tilde{H}^\top(I - \tilde{H})) \right) \quad (60)$$

$$\dot{\tilde{M}} = \tilde{M}\Omega_\times + \frac{k_2}{\gamma^3} \mathbb{P}(\tilde{H}^\top(I - \tilde{H})). \quad (61)$$

Consider the Lyapunov function

$$\mathcal{L} = \frac{1}{2} \|\tilde{H} - I\|^2 + \frac{1}{2k_2} \|\tilde{M}\|^2.$$

Differentiating  $\mathcal{L}$ , one obtains

$$\begin{aligned} \dot{\mathcal{L}} &= \text{tr} \left( (\tilde{H} - I)^\top \tilde{H} \left( \frac{1}{\gamma^3} \tilde{M} - \frac{1}{3\gamma^3} \text{tr}(\tilde{M})I \right. \right. \\ &\quad \left. \left. + k_1 \mathbb{P}(\tilde{H}^\top(I - \tilde{H})) \right) \right) \\ &\quad + \frac{1}{k_2} \text{tr} \left( \tilde{M}^\top \left( \tilde{M}\Omega_\times + \frac{k_2}{\gamma^3} \mathbb{P}(\tilde{H}^\top(I - \tilde{H})) \right) \right) \\ &= -k_1 \|\mathbb{P}(\tilde{H}^\top(I - \tilde{H}))\|^2. \end{aligned}$$

Using the assumption that  $\gamma \geq \epsilon$ ,  $\dot{\mathcal{L}}$  is uniformly continuous in time and Barbalat's lemma yields that  $\mathbb{P}(\tilde{H}^\top(I - \tilde{H})) \rightarrow 0$ .

Analogously to the arguments in the proof of Theorem 5.4, it can be shown that  $\tilde{H} \rightarrow 0$ . It follows that  $\tilde{M} \rightarrow \frac{1}{3} \text{tr}(\tilde{M})I$ . It is easily verified that  $\tilde{M}$  is uniformly continuous since  $\Omega$  is uniformly continuous, and it follows that  $\|\tilde{M} - \rho(t)I\| \rightarrow 0$  where  $\rho(t)$  is a time-varying scalar. However, recalling the error dynamics and applying the limit for  $\tilde{M}$ , one has equally that  $\|\tilde{M} - \frac{1}{3} \text{tr}(\tilde{M})\Omega_\times\| \rightarrow 0$ . Since  $\Omega$  is persistently exciting, these two limits can only hold if  $\rho(t) \rightarrow 0$  and  $\text{tr}(\tilde{M}) \rightarrow 0$ . Given that  $\tilde{M} \rightarrow \frac{1}{3} \text{tr}(\tilde{M})I$ , then  $\tilde{M} \rightarrow 0$ . We conclude that  $(\tilde{H}, \tilde{M})$  converges to either  $E_s$  or  $E_u$ . Finally, it is easily verified that the linearisation of the error system at  $E_s = (I, 0)$  is uniformly observable.  $\square$

**Remark 3:** In the case where  $V=0$  the orientation of target plane is unobservable, as discussed after Theorem 5.4. However, since Corollary 5.5 only attempts to identify  $\tilde{M}=0$ , the loss of observability of the structure parameters of the homography does not affect the convergence of the overall homography estimate.

**Remark 4:** Note that the continuity and persistence of excitation of  $\Omega$  are essentially required to insure that  $\tilde{M}=0$  and to guarantee the observability of

the system. The loss of continuity and persistence of excitation of  $\Omega$  does not affect the convergence of the homography error to identity as long as  $\Omega$  is upper bounded.

## 5.2 Constant linear velocity in the inertial-frame

In this subsection we consider the case where the linear velocity is an unknown constant in the *inertial* while the angular velocity in the body-fixed frame is measured. This is a less common scenario in robotics applications, however, it is a key scenario in the image registration and stabilisation problem (Irani et al. 1994; Buehler et al. 2001; Cho et al. 2007).

The assumption that the inertial velocity is constant leads to poorly defined asymptotic observability conditions on the homography system. A fixed inertial linear velocity must lead to one of: constant motion towards the observed plane, constant motion parallel to the plane or constant motion away from the observed plane. In the first case, the camera will intersect the target plane in a finite time, leading to a singularity in the homography representation. In the third case, the camera will move infinitely far away from the target plane, with the homography converging asymptotically to a pure rotation, leading to a loss of observability of the scene parameters in the asymptotic analysis of the filter. Only when the constant motion is parallel to the plane then the filter problem remain well-defined asymptotically. Nevertheless, it is often the case that a filter is used only for a short period of time, or that the constant velocity assumption is used when actually the velocity is slowly varying with time. The practical applications lead us to propose a filter for the case where the inertial velocity is assumed to be constant, however, we only prove a restricted result.

**Corollary 5.6:** Consider a camera moving with kinematics (37) and (38) viewing a planar scene (Assumption 5.1). Let  $H : \mathcal{B} \rightarrow \mathcal{A}$  denote the calibrated homography (40) (Assumption 5.2). Assume that the body-fixed frame velocities  $\Omega = {}^B_A\Omega_B$  is measured, uniformly continuous and bounded. Assume that the inertial linear velocity is constant

$${}^A V_B = \text{const.}$$

Let  $\hat{H}$  be given by (58) and

$$\dot{\hat{M}} = [\hat{M}, \Omega_\times] - \frac{k_2}{\gamma^3} \mathbb{P}(\tilde{H}^\top(I - \tilde{H})).$$

Then  $\mathbb{P}(\tilde{H}^\top(I - \tilde{H})) \rightarrow 0$ .



**Proof:** Given that  ${}^A V_B^A$  is constant, then  $V = {}^B V_B^A = {}^B R_A {}^A V_B^A$  and  $\dot{V} = -\Omega_\times V$ . Let  $M = (1/d_A)Vn_B^\top$  then it follows that

$$\dot{M} = -\Omega_\times M + M\Omega_\times = [M, \Omega_\times].$$

Noting that  $\text{tr}(\tilde{M}^\top[\tilde{M}, \Omega_\times]) = \text{tr}(\tilde{M}\Omega_\times\tilde{M}^\top - \tilde{M}^\top\Omega_\times\tilde{M}) = 0$  then the remainder of the proof is analogous to the proof (up to the point  $\mathbb{P}(\tilde{H}^\top(I - \tilde{H})) \rightarrow 0$ ) in Corollary 5.5.  $\square$

## 6. Conclusion

In this article, we proposed a nonlinear complementary filter on the special linear  $SL(3)$ . The filter obtained has a natural complementary filtering interpretation, preserving the low-frequency component of the state measurement and fusing this with the high-frequency content of the integrated velocity measurement. The simple case where the group velocity is known is considered and then extended to a filter that estimates an unknown constant group velocity. Motivated by the homography example, we also consider the case where the angular velocity of the camera is measured and the scene is static or moving with constant velocity, a common scenario in de-noising of sequences, image registration problems and compensating for video ‘shake’ as well as estimation of homographies for navigation of aerial vehicles. We prove almost global stability and local exponential stability of the filters considered and believe that the filters provide a robust and effective solution to the considered problems.

## Acknowledgements

This research was supported by the Australian Research Council through discovery grant DP0987411 ‘State Observers for Control Systems with Symmetry’ and the ANR-PSIRob project SCUAV ‘Sensory Control of Unmanned Aerial Vehicles’.

## Notes

1. Here we use the fact that  $v$  is an eigenvector of  $\tilde{H}$  with eigenvalue  $1/\lambda^2$  and that  $Zv$  is orthogonal to  $v$ , and hence is also an eigenvector of  $\tilde{H}$  but with eigenvalue  $\lambda$ .
2. Available for download at <http://esm.gforge.inria.fr>.
3. We reserve the upper left index to indicate what frame of reference a physical object is expressed with respect to. The right subscript refers to the object being measured, and the left subscript refers to the frame with respect to which the measurement is made. Thus the vector  ${}_A\xi_B$  representing the origin of  $\{B\}$  with respect to  $\{A\}$  can be expressed in  $\{A\}$  as  ${}_A\xi_B$  or in  $\{B\}$  as  ${}_B\xi_B = R^\top {}_A\xi_B$ , with  $R = {}_A R_B$  the normal attitude matrix representing the orientation of  $\{B\}$  with respect to  $\{A\}$ .
4. Where the  $\text{vec}$  operation stacks the columns of a matrix one on top of the other to form a vector and  $\otimes$  is the

Kronecker matrix product (see, e.g. Helmke and Moore 1994). Define  $I_n \in \mathbb{R}^{n \times n}$  to be an  $n$ -dimensional identity matrix,  $0_{n \times m} \in \mathbb{R}^{n \times m}$  the zero matrix and  $\mathbb{T} \in \mathbb{R}^{9 \times 9}$  to be the permutation matrix such that  $\mathbb{T} \text{vec}(X) = \text{vec}(X^\top)$ .

## References

- Benhimane, S., and Malis, E. (2007), ‘Homography-based 2D Visual Tracking and Servoing’, *International Journal of Robotic Research*, 26, 661–676.
- Bonnabel, S., Martin, P., and Rouchon, P. (2008a), ‘Symmetry-preserving Observers’, *IEEE Transactions on Automatic Control*, 53, 2514–2526.
- Bonnabel, S., Martin, P., and Rouchon, P. (2008b), ‘Nonlinear Observer on Lie Groups for Leftinvariant Dynamics with Right-left Equivariant Output’, in *Proceedings of the 17th World Congress The International Federation of Automatic Control*, July 6–11, Seoul, Korea.
- Buehler, C., Bosse, M., and McMillan, L. (2001), ‘Non-metric Image-based Rendering for Video Stabilisation’, in *Proceedings of the 2001 IEEE Computer Society Conference on Computer Vision and Pattern Recognition (CVPR)*, Vol. 2, pp. II-609–II-614.
- Caballero, F., Merino, L., Ferruz, J., and Ollero, A. (2007), ‘Homography Based Kalman Filter for Mosaic Building. Applications to UAV Position Estimation’, in *IEEE International Conference on Robotics and Automation*, April, pp. 2004–2009.
- Cho, W., Kim, D., and Hong, K. (2007), ‘Affine Motion Based CMOS Distortion Analysis and CMOS Digital Image Stabilization’, *IEEE Transactions on Consumer Electronics*, 53, 833–841.
- Deguchi, K. (1998), ‘Optimal Motion Control for Image-based Visual Servoing by Decoupling Translation and Rotation’, in *Proceedings of the International Conference on Intelligent Robots and Systems*, pp. 705–711.
- Dellaert, F., Thorpe, C., and Thrun, S. (1998), ‘Super-resolved Texture Tracking of Planar Surface Patches’, in *Proceedings of the 1998 EEWRSJ International Conference on Intelligent Robots and Systems*, October, Victoria, BC, Canada.
- Dias, J., Vinzce, M., Corke, P., and Lobo, J. (2007), ‘Editorial: Special Issue: 2nd Workshop on Integration of Vision and Inertial Sensors’, *International Journal of Robotic Research*, 26, 515–517.
- Fang, Y., Dixon, W., Dawson, D., and Chawda, P. (2005), ‘Homography-based Visual Servoing of Wheeled Mobile Robots’, *IEEE Transactions on Systems, Man, and Cybernetics – Part B*, 35, 1041–1050.
- Faugeras, O., and Lustman, F. (1988), ‘Motion and Structure from Motion in a Piecewise Planar Environment’, *International Journal of Pattern Recognition and Artificial Intelligence*, 2, 485–508.
- Fraundorfer, F., Engels, C., and Nister, D. (2007), ‘Topological Mapping, Localization and Navigation using Image Collections’, in *IEEE/RSJ International Conference on Intelligent Robots and Systems (IROS)*, October 29–November 2, pp. 3872–3877.

- Hartley, R., and Zisserman, A. (2000), *Multiple View Geometry in Computer Vision* (2nd ed.), Cambridge, MA: Cambridge University Press.
- Helmke, U., and Moore, J.B. (1994), 'Optimization and Dynamical Systems', *Communications and Control Engineering*, London, UK: Springer-Verlag.
- Hol, J., Schn, T., and Gustafsson, F. (2010), 'Modeling and Calibration of Inertial and Vision Sensors', *The International Journal of Robotics Research*, 29, 231–244.
- Irani, M., Rousso, B., and Peleg, S. (1994), 'Recovery of Ego-motion using Image Stabilisation', in *IEEE Computer Society Conference on Computer Vision and Pattern Recognition (CVPR)*, pp. 454–460.
- Khalil, H.K. (1996), *Nonlinear Systems* (2nd ed.), New Jersey, USA: Prentice Hall.
- Lageman, C., Mahony, R., and Trumf, J. (2008), 'State Observers for Invariant Dynamics on a Lie Group', in *Proceedings of the International Symposium on Mathematical Theory of Networks and Systems (MTNS)*, 8pp.
- Lageman, C., Trumf, J., and Mahony, R. (2010), 'Gradient-like Observers for Invariant Dynamics on a Lie Group', *IEEE Transactions on Automatic Control*, 55, 367–377.
- Lobo, J., and Dias, J. (2007), 'Relative Pose Calibration Between Visual and Inertial Sensors', *The International Journal of Robotics Research*, 26, 561–575.
- Ma, Y., Soatto, S., Kosecka, J., and Sastry, S. (2003), *An Invitation to 3-D Vision: From Images to Geometric Models*, New York, USA: Springer-Verlag.
- Mahony, R., Hamel, T., and Pflimlin, J.M. (2008), 'Nonlinear Complementary Filters on the Special Orthogonal Group', *IEEE Transactions on Automatic Control*, 53, 1203–1218.
- Malis, E., Chaumette, F., and Boudet, S. (1999), '2-1/2-D Visual Servoing', *IEEE Transactions on Robotics and Automation*, 15, 238–250.
- Malis, E., Hamel, T., Mahony, R., and Morin, P. (2009), 'Dynamic Estimation of Homography Transformations on the Special Linear Group for Visual Servo Control', in *Proceedings of the IEEE International Conference on Robotics and Automation (ICRA)*, Kobe, Japan, pp. 1498–1503.
- Malis, E., Hamel, T., Mahony, R., and Morin, P. (2010), 'Estimation of Homography Dynamics on the Special Linear Group', in *Visual Servoing via Advanced Numerical Methods* (chap. 8), eds. G. Chesi, and K. Hashimoto, Springer, pp. 139–158.
- Malis, E., and Vargas, M. (2007), 'Deeper Understanding of the Homography Decomposition for Vision-based Control', Technical report Research Report 6303, Institute National de Reserche en Informatique et en Automatique, INRIA.
- Martin, P., and Salaün, E. (2008), 'An Invariant Observer for Earth-velocity-aided Attitude Heading Reference Systems', in *Proceedings of the 17th World Congress The International Federation of Automatic Control*, July 6–11, Seoul, Korea.
- Martinelli, A. (2012), 'Vision and IMU Data Fusion: Closed-form Solutions for Attitude, Speed, Absolute Scale, and Bias Determination', *IEEE Transactions on Robotics*, 28, 44–60.
- Mondragóon, I., Campoy, P., Martínez, C., and Olivares-Méndez, M. (2010), '3D Pose Estimation Based on Planar Object Tracking for UAVs Control', in *IEEE International Conference on Robotics and Automation (ICRA)*, May, Anchorage.
- Mufti, F., Mahony, R., and Kim, J. (2007), 'Super Resolution of Speed Signs in Video Sequences', *Digital Image Computing: Techniques and Applications (DICTA)*, December, Adelaide, Australia.
- Scaramuzza, D., and Siegwart, R. (2008), 'Appearance-guided Monocular Omnidirectional Visual Odometry for Outdoor Ground Vehicles', *IEEE Transactions on Robotics*, 24, 1015–1026.
- Tayebi, A., and McGilvray, S. (2006), 'Attitude Stabilisation of a VTOL Quadrotor Aircraft', *IEEE Transactions on Control Systems Technology*, 14, 562–571.
- Vasconcelos, J., Cunha, R., Silvestre, C., and Oliveira, P. (2010), 'A Nonlinear Position and Attitude Observer on SE(3) using Landmark Measurements', *Systems & Control Letters*, 59, 155–166.
- Wang, H., Yuan, K., Zou, W., and Zhou, Q. (2005), 'Visual Odometry Based on Locally Planar Ground Assumption', in *Proceedings of the 2005 IEEE International Conference on Information Acquisition*, Hong Kong and Macau, China.
- Zhang, B., Li, Y., and Wu, Y. (2007), 'Self-recalibration of a Structured Light System via Planebased Homography', *Pattern Recognition*, 40, 1368–1377.